



VISIBLE LIGHT DRIVEN PHOTOCATALYTIC DEGRADATION OF PARACETAMOL USING INCENSE ASH SUPPORTED ZnO NANOCOMPOSITES

(Degradasi Paracetamol secara Pemangkinan Foto dengan Penggunaan Komposit Nano ZnO
berdasarkan Abu Kemenyan)

Pei Teng Lum*, Keng Yuen Foo, Nor Azazi Zakaria

*River Engineering and Urban Drainage Research Centre (REDAC), Engineering Campus,
Universiti Sains Malaysia, 14300 Nibong Tebal, Penang, Malaysia*

*Corresponding author: peiteng1013@gmail.com

Received: 10 July 2019; Accepted: 3 September 2019

Abstract

In this work, the preparation of a newly synthesized incense ash (IA) supported zinc oxide (ZnO) nanocomposite has been attempted using a simple physical coating method. The physical and chemical properties of the nanocomposite were examined by using scanning electron microscopy (SEM), Fourier Transform Infrared Spectroscopy (FT-IR) and pore structural analysis. The photocatalytic activity was examined by performing the batch photocatalytic degradation of paracetamol (PCM). The preparation and experimental parameters including the ash impregnation ratio, catalyst loadings, initial PCM concentration and irradiation time were accessed. Morphological study revealed that highly porous structure of IA provides a suitable supporting surface area for the better deposition of ZnO to offer the enhanced adsorption and photodegradation reaction. A complete degradation with the high concentration of 50 mg/L was achieved within 3.5 hours. High stability of synthesized nanocomposite was demonstrated from the reusability test, with higher than 95% of removal even after five successive regeneration cycles. The present study provides an efficient photocatalytic degradation route by IA supported ZnO nanocomposite in PCM treatment, one of the emerging pollutants in wastewater effluents.

Keywords: incense ash, nanocomposites, paracetamol, photodegradation

Abstrak

Dalam kajian ini, penyediaan komposit nano zink oksida (ZnO) berdasarkan abu kemenyan (IA) melalui teknik salutan fizikal telah dicuba. Ciri-ciri fizikal dan kimia komposit nano telah dikendalikan dengan menggunakan mikroskop imbasan elektron (SEM), Spektroskopi Infamerah Transformasi Fourier (FT-IR) dan analisis keliangan. Prestasi pemangkinan foto diuji dengan degradasi foto bagi paracetamol (PCM). Parameter penyediaan dan eksperimen termasuk nisbah jerap abu, dos pemangkin, kepekatan asal pewarna dan masa penyinaran telah dikaji. Kajian morfologi permukaan menunjukkan struktur IA yang berliang sesuai untuk dijadikan permukaan sokongan bagi pemendapan ZnO yang lebih lengkap dan menawarkan kecekapan tindak balas pemangkinan foto. Degradasi yang sempurna dengan kepekatan asal 50 mg/L dicapai dalam masa 3.5 jam. Ketahanan komposit nano ini yang tinggi telah ditunjukkan dari ujian penggunaan semula, dengan kecekapan degradasi foto yang melebihi 95% walaupun selepas lima kitaran penggunaannya. Kajian ini menzahirkan laluan degradasi pemangkinan foto yang cekap dengan penggunaan komposit nano ZnO berdasarkan IA dalam perawatan PCM, salah satu bahan pencemar yang muncul dalam efluen air sisa.

Kata kunci: abu kemenyan, komposit nano, paracetamol, degradasi foto

Introduction

Paracetamol (PCM), chemically named as acetaminophen, 4-hydroxyacetamide, 4-acetamidophenol or N-(4-hydroxyphenyl) acetamide, is a synthetic derivative of p-aminophenol with analgesic and antipyretic activity. It is an over-the-counter drug which most widely used for fever or pain relief worldwide. As the consequences of huge production and quantitative use of PCM, it is ubiquitous with a concentration up to 10 mg/L in the influents and effluents of wastewater treatment plants (WWTP), and in the range of 10 to 100 ng/L in surface water [1]. Besides, the presence of PCM has been recorded up to a concentration of 0.5 to 45 ng/L in drinking water and 4.1 to 73 ng/L in the freshwater river systems [2]. Untreated PCM is poorly biodegradable due to its complex molecular structure, and their chemically persistent.

To the best of our knowledge, despite there are no legally permissible limits for the existence of PCM in waste effluents, the effect of “chronic exposure to low dose” is still uncertain for human health, owing to findings have revealed that pharmaceuticals compounds are pharmacologically active and toxic in nature. They are genotoxicity, resistant to the microorganism, and long-term ingestion of these compounds through drinking water will lead to their bioaccumulation in bodies, potentially detrimental to human health [3]. For remediation, conventional WWTP consisted of the biological treatment process and physical-chemical process including adsorption, reverse osmosis, coagulation, flocculation, and filtration is inefficient to remove PCM completely, because these treatment techniques are not designed to treat these refractory micro-pollutants contaminated water. Predominantly, physical process sorely characterized by phase transfer of pollutants without degradation while biological treatment merely limited to biodegradable compounds containing wastewater [4].

Keeping in view above, the necessity of priority attention to identifying the reliable, efficient and eco-friendly techniques for the elimination of pharmaceuticals compounds is highlighted. In recent year, heterogeneous photocatalysis is gaining a considerable interest as a promising avenue in pharmaceuticals contaminants, owing to chemical stability, relatively low cost and non-toxicity [4]. It is characterized by the generation of reactive oxygen species (ROS), non-selectively to oxidize the recalcitrant contaminants through a complete mineralization into the carbon dioxide and water without producing secondary waste in the environment [5]. Among a variety of semiconductor photocatalyst, TiO₂ and ZnO are most widely used for the photocatalytic process in drugs contaminated water. Research on photodegradation of PCM have been studied using different doping contents and different morphologies of TiO₂ and ZnO. However, hitherto, there is a paucity of literature on the utilization of ash based photocatalyst on the photodegradation of PCM.

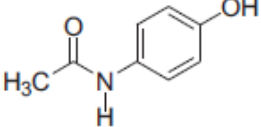
In the perspective, incense ash (IA), a waste by-product from incense burning, it is highly generated in Asian countries including Malaysia, Singapore, Thailand, China, Taiwan and Japan. Among Asian community, incense burning is not only a traditional practice for religious festivals in temples but also a long lasting daily practice in-house as paying respect to their ancestors [6]. In this case, daily generation of incense ash as longer time might contribute to the environmental problem if proper disposal is not implemented. It is noteworthy that many studies have been documented on the synthesis and photocatalytic activity of fly ash supported nanocomposite, in which ash is reported effective for the removal of certain pollutants [7]. Herein, a considerable interest is gained to develop a novel IA supported ZnO nanocomposite for the degradation of PCM. Morphological, functional and surface characterization were investigated. The effect of ash impregnation ratio, catalyst loadings, initial concentration and irradiation time on photocatalytic process were examined. The reusability of the prepared nanocomposite was also elucidated.

Materials and Methods

Model pollutants

Paracetamol (PCM), a pain relief drug was chosen as the model organic pollutant in this study. The chemical structure and physio-chemical properties of PCM are as given (Table 1). A standard stock solution with the concentration of 50 mg/L was prepared in deionized water. The working solutions were prepared by diluting the stock solution successively.

Table 1. Chemical structure and physiochemical properties of PCM

Compound	Chemical Structure	Molecular Weight (g mol ⁻¹)	pKa	λ max (nm)
Paracetamol (PCM)		151.7	9.4	248.8

Preparation of photocatalytic nanocomposite

Incense ash (IA), a by-product of incense burning was chosen as the initial raw precursor. The collected IA was washed thoroughly with deionized water to remove adhering dirt particles, dried and sieved to the particles size of 250-500 μm. In the modification process, IA was basic functionalized with 1M of sodium hydroxide solution. The modified IA was rinsed with a copious amount of deionized water till a constant pH was acquired in the washing solution and dried at 80 °C. The ZnO/IA nanocomposite was prepared by using a simple physical coating method. A requisite amount of ZnO pure powder were mixed thoroughly with modified IA in the impregnation ratio (ZnO: IA) of 1:1 to 1:5 kept in air-tight bottles for further analysis.

Characterization

Scanning Electron Microscopy (SEM, Zeiss Supra 35 VP, Germany) was performed to visualize the surface morphology. The surface functional groups were specified by Fourier Transform Infrared (FTIR) Spectroscopy (FTIR-2000, PerkinElmer) using KBr pellet method, in the scanning range of 4000–400 cm⁻¹. The surface physical properties of nanocomposites were specified by nitrogen adsorption–desorption isotherm at 77 K using an automatic Micromeritics ASAP 2020 volumetric adsorption analyzer. Prior to the gas adsorption measurement, the samples were degassed for 8 h at 573 K under a vacuum condition. The application of Brunauer-Emmett-Teller (BET) was applied to calculate the specific surface area, whereas the micropore surface area, external surface area, and micropore volume were accessed by using the t-plot method.

Photocatalytic study

The photocatalytic experiments were conducted in self-assembled photoreactor, consisting of a cylindrical flask equipped with four visible light sources, circulating water jackets and a cooling fan. In a typical test, a prefixed amount of photocatalyst was dispersed into 100 mL of PCM solution. Prior to irradiation, all mixture was stirred in darkness for 30 minutes to achieve adsorption-desorption equilibrium. Aliquots were withdrawn at a specific time for each experiment and filtered using a syringe filter (Nylon Millipore 0.25 μm) prior to analysis to minimize the interference of powdered catalyst with the analysis. The concentration of PCM solution was determined using UV-Vis spectrophotometer (UV-1800 Shimadzu, Japan) at 243 nm. The degradation efficiency of PCM can be expressed by the following equation:

$$\text{Degradation rate (\%)} = \frac{C_0 - C_t}{C_0} \times 100 \quad (1)$$

where C_0 and C_t referred to the initial concentration of PCM and at time t .

The effects of catalyst loading, initial concentration and irradiation time on the photocatalytic performances of PCM was evaluated. All the experimental run was conducted in duplicate and the average values were reported. The reusability test was conducted with five successive degradation cycles of PCM at the initial concentration of 10 mg/L under the optimized experimental condition. For each regeneration process, the nanocomposite was filtered, washed with deionized water till the constant pH acquired for the washing solution, and dried at 120 °C for 1 hour. The regenerated nanocomposite was reutilized for the next consecutives degradation run.

Results and Discussion

Preparation of IA supported ZnO nanocomposite

The variation of photocatalytic performances of IA supported nanocomposite at different ash impregnation ratio were accessed, as presented in Figure 1. It can be clearly seen that the ZnO/IA nanocomposites exhibited a comparatively higher PCM degradation efficiency of 36% to 57%, as compared with the degradation rate of only 2.7% and 30% for the raw IA and pure ZnO, respectively. The result is mainly attributed to the principle of a kind of synergy was induced between IA and ZnO, introducing their bifunctional properties of adsorption and photocatalysis [8]. An increase of the availability of surface binding sites for the targeted PCM, induce a higher migration of adsorbed PCM to photoactive center of ZnO, as well as increase the rate of the photocatalytic process [9]. Another reason can be explained by IA improve the dispersion of nanocomposite in PCM solution and increase the photons reach the surface of the catalyst, in turn enhancing the utilization of visible light for photocatalysis [10].

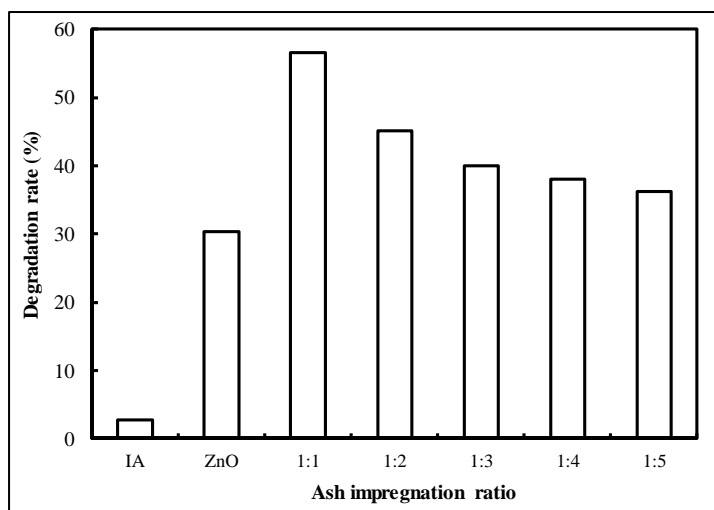


Figure 1. Effect of ash impregnation ratio (ZnO:IA) on the photodegradation of PCM (catalyst loading = 1.0 g/100 mL, $C_0 = 50$ mg/L; $t = 60$ minutes)

The removal of PCM was greatly enhanced with the addition of IA, however, the degradation efficiency was gradually decreased beyond the optimal impregnation ratio of 1:1. This observation can be assigned to an excessive loading of IA that turned unfavorable to the photocatalytic reaction, due to agglomeration of ash particles within the photocatalytic nanoparticles, which confine the path of the light from reaching to the ZnO photocatalyst. These phenomenon result in the lower formation of photo-induced electron-hole pairs and in turn inhibit the photocatalytic activity of the nanocomposite [11]. Therefore, the optimum ash impregnation ratio of 1:1 was applied for the further experiments.

Characterization

The surface morphology of IA, ZnO, ZnO/IA nanocomposite were visualized by the scanning electron micrographs (SEM), with a magnification of 500x, as displayed in Figure 2. Generally, the pristine ZnO (Figure 2a) exhibited a homogeneous surface, consisted of mainly a series of unique flower-like nanoparticles, with each nanoparticle were formed by a complex configuration of nanorods. Similar structure has been observed by Pant et al. [12] during the synthesis ZnO. The SEM image of raw IA exhibited a rough and highly porous structure, with the irregular distribution of spherical shaped particles. Conversely, the ZnO/IA nanocomposite revealed the dispersion of numerous clusters of ZnO derived nanoparticles over the spherical-shaped surface, to be filled inside the air holes of IA. This current finding indicates the successive deposition of ZnO nanoparticles onto the ash surface by using a simple physical coating technique. The morphological characterization has verified that these newly prepared nanocomposites are undoubtedly serve for a greater adsorptive and catalytic surface active site, to induce a higher generation of hydroxyl radicals in related to the absorption of greater photon energy, that in turn enhance the

synergistic adsorption from ash support and photocatalytic activity from photocatalyst for the effective degradation of PCM.

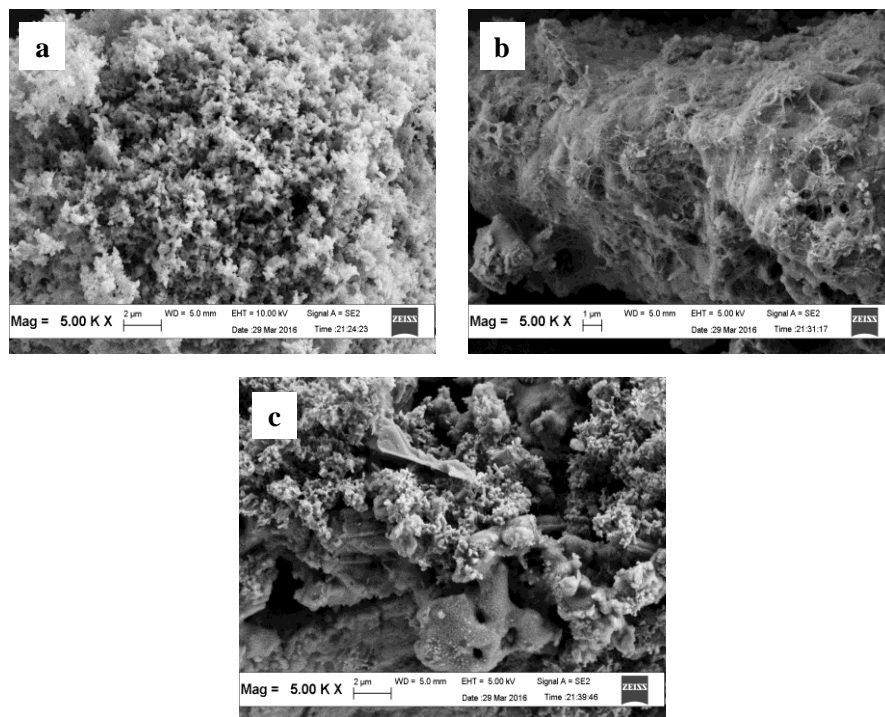


Figure 2. Scanning electron micrographs of (a) ZnO, (b) IA, and (c) ZnO/IA nanocomposite

The surface physical properties of IA, ZnO and ZnO/IA nanocomposite are given in Table 2. As shown in the table, the BET surface area, Langmuir surface area and total pore volume of ZnO and raw IA were obtained to be 5.78 m²/g and 12.72 m²/g; 7.51 m²/g and 16.15 m²/g; 0.012 cm³/g and 0.043 cm³/g, respectively. As compared with ZnO and IA, ZnO/IA nanocomposite demonstrated an enhanced BET surface area, Langmuir surface area and total pore volume with 17.67 m²/g, 21.54 m²/g, and 0.046 cm³/g, respectively. Notably, positive development was observed for the surface porosity of composite, suggesting that IA serves as an ideal absorbent to provide a larger surface area for the deposition of ZnO, as well as increases the surface area of whole matrix [13].

Table 2. Surface physical characteristics of ZnO, IA, and ZnO/IA nanocomposite

Properties	ZnO	IA	ZnO/IA
BET surface area (m ² /g)	5.78	12.72	17.67
Langmuir surface area (m ² /g)	7.51	16.15	21.54
External surface area (m ² /g)	6.31	12.30	16.64
Micropore surface area (m ² /g)	0.53	0.42	1.83
Total pore volume (cm ³ /g)	0.012	0.043	0.046

The FTIR spectra of the ZnO, IA and ZnO/IA derived nanocomposite are presented in Figure 3, respectively. The broad band at 3446-3422 cm⁻¹ is attributed to the stretching of O-H bonds. The region between 2924-2513 cm⁻¹ is assigned to the stretching vibration of C-H bond. The signals at 1798 cm⁻¹ is ascertained to the stretching vibration of C=O. The adsorption transmittance at 1427/1424 is ascribed to the symmetrical stretching of Si-O-Si bond,

whereas $1012\text{-}1008\text{ cm}^{-1}$, 874 cm^{-1} and $480/475\text{ cm}^{-1}$ refer to the bending vibration of Si-O bond. The new peaks at 712 cm^{-1} on the FT-IR spectra of IA and ZnO/IA nanocomposite is pointing to the bending modes of COO-, indicating the presence of calcite (CaCO_3) [14]. On the other hand, the transmittance at $543/524\text{ cm}^{-1}$ and 439 cm^{-1} are denoted to the stretching vibration of Zn-O. The alteration between the IA and ZnO/IA nanocomposite, in terms of lower intensity and deconvolution of peaks has verified the homogeneous deposition of ZnO onto the surface of IA, *via* Van der Waals interaction over the matrix surfaces [15]. Such interactions have been reported in the TiO_2 -deposited fly ash derived nanocomposite [16].

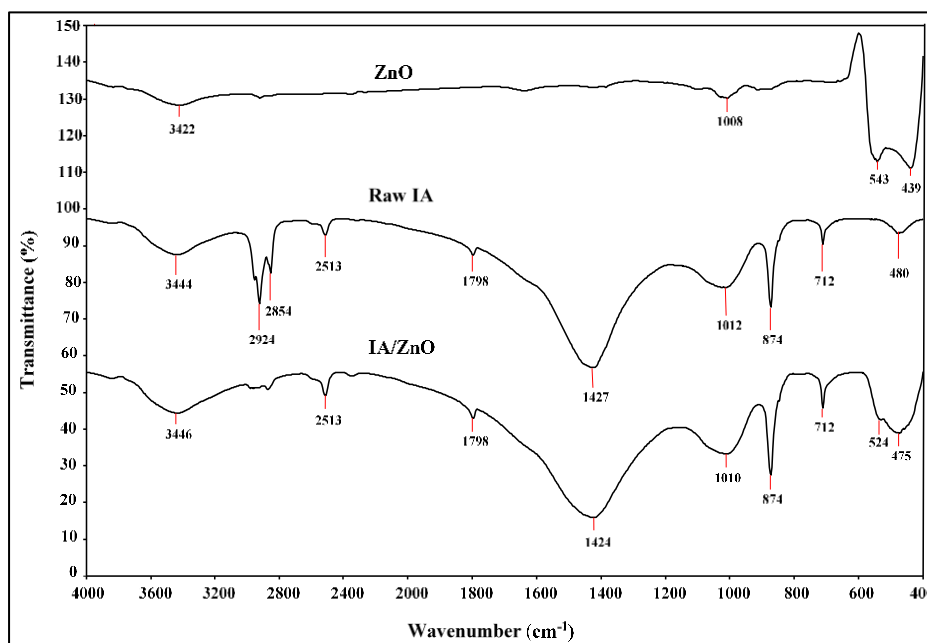


Figure 3. Fourier-Transform Infrared spectra of ZnO, IA, and ZnO/IA nanocomposite

Photocatalytic performances: Effect of catalyst loading

Catalyst loading is the major influencing parameter affecting the operation cost, and the feasibility for the large-scale practical applications. The effect of catalyst loading on the photocatalytic degradation of PCM was examined by varying the catalyst loading from $1.0\text{ g}/100\text{ mL}$ to $2.0\text{ g}/100\text{ mL}$, as displayed in the Figure 4. Obviously, increasing the catalyst loading showed a decrement on the degradation process. The degradation efficiency of PCM decreased linearly from 57 % to 41%, with an increase of catalyst loading from $1.0\text{ g}/100\text{ mL}$ to $2.0\text{ g}/100\text{ mL}$. At the optimal catalyst loading of $1.0\text{ g}/100\text{ mL}$, the superior enhancement of PCM removal was achieved. The result is ascribed to the larger availability of surface absorption sites that favoring towards more PCM molecules adsorb on the catalyst surface [17]. As well, the higher number of surface catalytic sites at the optimal catalyst loading may contribute to the higher photons absorption to promote a greater formation of photogenerated hydroxyl radicals, in turn enhancing the photocatalytic reaction of PCM [18].

Beyond the catalyst loading of $1.0\text{ g}/100\text{ mL}$, the rate of degradation decreased markedly and remained constant at approximately 42% as the catalyst amount further increased from $1.6\text{ g}/100\text{ mL}$ to $2.0\text{ g}/100\text{ mL}$. Similar phenomenon was reported by Hu et al. [19] in the photodegradation of PCM by BiVO_4 catalyst. This finding is associated with the addition of excess catalyst above the saturation limit that might induce the dispersion of agglomerated catalyst particles, cripple the transparency of the PCM solution, which further reduce light penetration into the solution [20]. Consequently, a decrease of the number of photo-generated electron-hole pairs retard the degradation efficiency of PCM. This present study suggested a good balance between the catalyst loading with the tested pollutants should be well optimized to avoid superfluous catalyst usage.

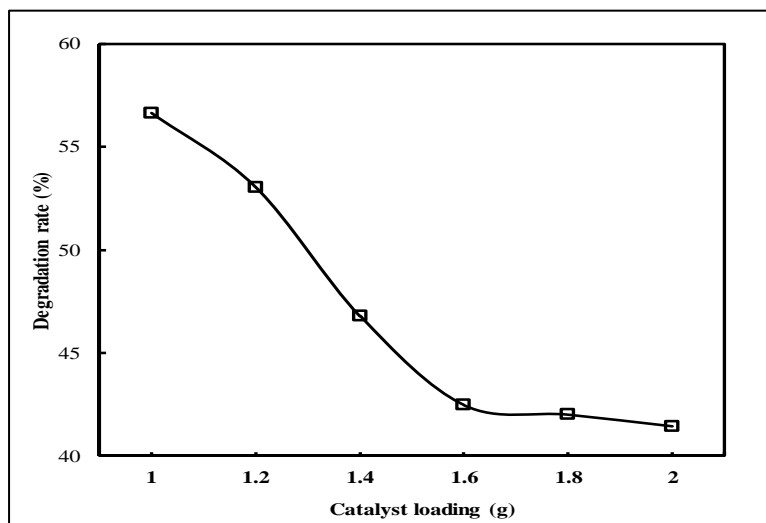


Figure 4. Effect of catalyst loading on the photodegradation of PCM ($C_0 = 50$ mg/L; $t = 60$ minutes)

Effect of initial concentration and irradiation time

The variation of PCM removal with respect to irradiation time, at the initial concentration of 10 mg/L to 50 mg/L under the optimized experimental conditions are depicted in Figure 5. In this study, increasing the initial concentration of PCM from 10 mg/L to 50 mg/L demonstrated a rising of irradiation time from 28 minutes to 210 minutes for the complete degradation of PCM. At lower concentration of PCM, the active sites on the catalyst surface are enough for the adsorption of PCM and water molecules to induce rapid oxidation process [18].

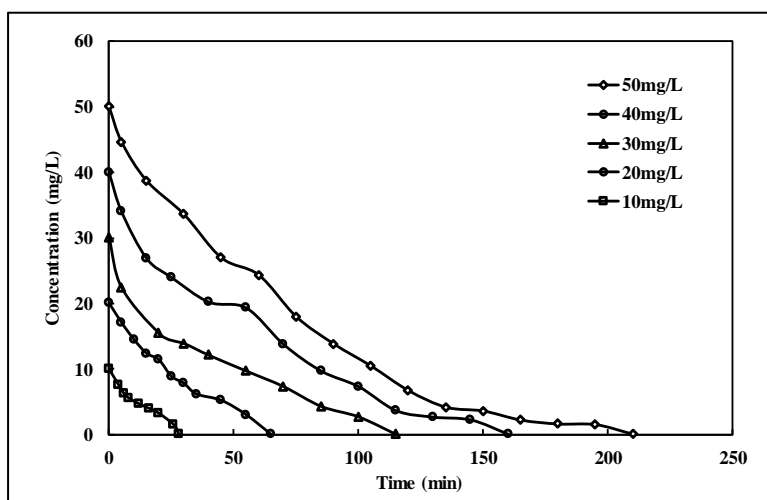


Figure 5. Plot of degradation of PCM as a function of initial concentrations and irradiation time

Conversely, additional PCM molecules that adsorbed onto the surface of the catalyst when the PCM were overloaded triggers to a saturation and deactivation of surface active. This phenomenon induces an ineffective action of hydroxyl radicals for the photocatalytic reaction. Additionally, a higher initial concentration decreases the degree of light transmission in aqueous solution. Lesser light activation and formation of reactive species radicals throughout the photodegradation process directly reduce the photocatalytic activity of the photocatalyst. In this case,

the photolysis of PCM molecules rather than the photocatalysis might take place [21]. As its consequences, the removal rate would be rapidly retarded as the initial concentration increased.

Reusability study

Catalytic stability is another essential parameter of the photocatalytic process for cost-effective and long-term practical application. The reusability of the newly synthesized ZnO/IA nanocomposite was examined by performing five consecutive cyclic experiments using PCM, as depicted in Figure 6. The result clearly demonstrated the extremely stable photocatalytic ability of these nanocomposites, with the high removal above 95% for PCM even after five successive cycles. No apparent loss of photocatalytic activity of the nanocomposite can be explained by the structural integrity of the heterostructure of the nanocomposite is maintained, it is not easily photo corroded and deactivated against the photodegradation process [22].

Moreover, it is deduced that IA could serve as the adsorptive support to immobilize the dispersion of ZnO onto the adsorbent surface, to protect against the destruction of the surface binding catalytic sites. This hybrid adsorptive and degradation surface active sites have contributed to both adsorptive force and the generation of photoinduced reactive species for the effective photodegradation reaction [23]. Nevertheless, further recovery resulted in a slight decrease of the photocatalytic activity, mainly related to the blockage of the surface binding active sites of the nanocomposites, and the possible leaching of the surface fragment of the catalyst after several successive adsorption and photocatalytic reaction [24].

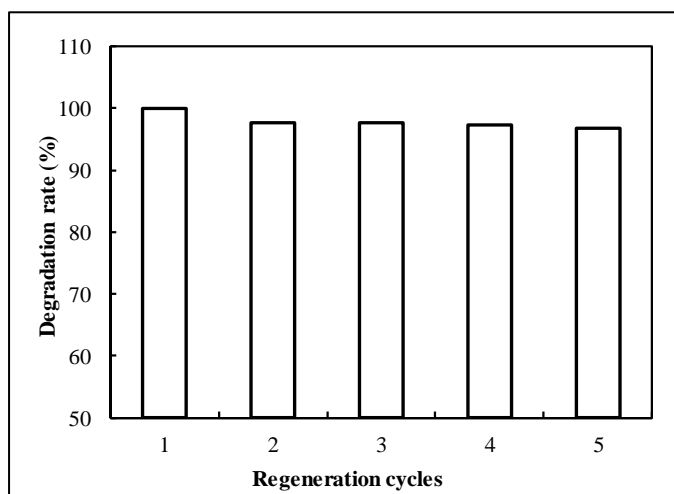


Figure 6. Reusability test of ZnO/IA nanocomposite for the photodegradation of PCM (catalyst loading = 1.0 g/100 mL, $C_0 = 10$ mg/L; $t = 30$ minutes)

Conclusion

This present study demonstrated that ZnO/IA nanocomposite have been successfully prepared, and it exhibited a good photocatalytic performance on the photodegradation of PCM under the optimized experimental conditions. The finding highlighted the alternative pathway and potentiality of incense ash to be a cost-effective supporting material for the preparation of a valuable photocatalytic nanocomposite. The synergistic effect of adsorption and photocatalysis from IA and ZnO, respectively, leading to an enhancement of the degradation of water contaminants. Therefore, several perspectives on the diverse applications for future research works are suggested. For the practicability, the photocatalytic activity of this newly prepared nanocomposite could be further examined for the on-site treatment of pharmaceutical effluents with multiple pollutants, instead of synthetic pharmaceuticals tested solution. Besides, the potential of other agricultural ash as the precursor for the preparation of low-cost photocatalyst could be explored.

Acknowledgement

The authors acknowledge the financial support provided by Universiti Sains Malaysia, under the USM Short Term grant scheme (Project No. 304/PREDAC/6315111).

References

1. Magureanu, M., Mandache, N. B. and Parvulescu, V. I. (2015). Degradation of pharmaceutical compounds in water by non-thermal plasma treatment. *Water Research*, 81: 124-136.
2. Gavrilescu, M., Demnerová, K., Aamand, J., Agathos, S. and Fava, F. (2015). Emerging pollutants in the environment: present and future challenges in biomonitoring, ecological risks and bioremediation. *New Biotechnology*, 32(1): 147-156.
3. Atanasov, A. G., Waltenberger, B., Pferschy-Wenzig, E.-M., Linder, T., Wawrosch, C., Uhrin, P., Temml, V., Wang, L., Schwaiger, S., Heiss, E. H., Rollinger, J. M., Schuster, D., Breuss, J. M., Bochkov, V., Mihovilovic, M. D., Kopp, B., Bauer, R., Dirsch, V. M. and Stuppner, H. (2015). Discovery and resupply of pharmacologically active plant-derived natural products: A review. *Biotechnology Advances*, 33(8): 1582-1614.
4. Mirzaei, A., Chen, Z., Haghighat, F., & Yerushalmi, L. (2016). Removal of pharmaceuticals and endocrine disrupting compounds from water by zinc oxide-based photocatalytic degradation: A review. *Sustainable Cities and Society*, 27: 407-418.
5. Kaur, A., Umar, A. and Kansal, S. K. (2016). Heterogeneous photocatalytic studies of analgesic and non-steroidal anti-inflammatory drugs. *Applied Catalysis A: General*, 510: 134-155.
6. Lung, S.-C. C. and Hu, S.-C. (2003). Generation rates and emission factors of particulate matter and particle-bound polycyclic aromatic hydrocarbons of incense sticks. *Chemosphere*, 50(5): 673-679.
7. Jarusiripot, C. (2014). Removal of reactive dye by adsorption over chemical pretreatment coal based bottom ash. *Procedia Chemistry*, 9: 121-130.
8. Ökte, A. N. and Karamanis, D. (2013). A novel photoresponsive ZnO-flyash nanocomposite for environmental and energy applications. *Applied Catalysis B: Environmental*, 142-143: 538-552.
9. Liu, S., Zhu, J., Yang, Q., Xu, P., Ge, J. and Guo, X. (2015). Preparation of SnO₂-TiO₂/fly ash cenospheres and its application in phenol degradation. *Photochemistry and Photobiology*, 91(6): 1302-1308.
10. Lv, J., Sheng, T., Su, L., Xu, G., Wang, D., Zheng, Z. and Wu, Y. (2013). N, S co-doped-TiO₂/fly ash beads composite material and visible light photocatalytic activity. *Applied Surface Science*, 284: 229-234.
11. Visa, M., Carcel, R. A., Andronic, L. and Duta, A. (2009). Advanced treatment of wastewater with methyl orange and heavy metals on TiO₂, fly ash and their mixtures. *Catalysis Today*, 144(1-2): 137-142.
12. Pant, H. R., Park, C. H., Pant, B., Tijing, L. D., Kim, H. Y. and Kim, C. S. (2012). Synthesis, characterization, and photocatalytic properties of ZnO nano-flower containing TiO₂ NPs. *Ceramics International*, 38(4): 2943-2950.
13. Kim, H. J., Joshi, M. K., Pant, H. R., Kim, J. H., Lee, E. and Kim, C. S. (2015). One-pot hydrothermal synthesis of multifunctional Ag/ZnO/fly ash nanocomposite. *Colloids and Surfaces A: Physicochemical and Engineering Aspects*, 469: 256-262.
14. Reig, F., Gimeno-Adelantado, J. V. and Moya Moreno, C. M. (2002). FTIR quantitative analysis of calcium carbonate (calcite) and silica (quartz) mixtures using the constant ratio method. Application to Geological Samples. *Talanta*, 58: 811-821.
15. Chai, B., Yan, J., Wang, C., Ren, Z. and Zhu, Y. (2017). Enhanced visible light photocatalytic degradation of Rhodamine B over phosphorus doped graphitic carbon nitride. *Applied Surface Science*, 391: 376-383.
16. Wang, B., Li, C., Pang, J., Qing, X., Zhai, J. and Li, Q. (2012). Novel polypyrrole-sensitized hollow TiO₂/fly ash cenospheres: Synthesis, characterization, and photocatalytic ability under visible light. *Applied Surface Science*, 258(24): 9989-9996.
17. Thejaswini, T. V. L., Prabhakaran, D. and Maheswari, M. A. (2016). Soft synthesis of Bi Doped and Bi-N co-doped TiO₂ nanocomposites: A comprehensive mechanistic approach towards visible light induced ultra-fast photocatalytic degradation of fabric dye pollutant. *Journal of Environmental Chemical Engineering*, 4(1): 1308-1321.
18. Mameri, Y., Debbache, N., Benacherine, M. E. M., Seraghni, N. and Sehili, T. (2016). Heterogeneous photodegradation of paracetamol using Goethite/H₂O₂ and Goethite/oxalic acid systems under artificial and natural light. *Journal of Photochemistry and Photobiology A: Chemistry*, 315: 129-137.

19. Hu, C., Xu, J., Zhu, Y., Chen, A., Bian, Z. and Wang, H. (2016). Morphological effect of BiVO₄ catalysts on degradation of aqueous paracetamol under visible light irradiation. *Environmental Science and Pollution Research*, 23(8):18421-18428.
20. Sheng, F., Zhu, X., Wang, W., Bai, H., Liu, J., Wang, P., Zhang, R., Han, L. and Mu, J. (2014). Synthesis of novel polyoxometalate K₆ZrW₁₁O₃₉Sn·12H₂O and photocatalytic degradation aqueous azo dye solutions with solar irradiation. *Journal of Molecular Catalysis A: Chemical*, 393: 232-239.
21. Soltani, R. D. C., Khataee, A. and Mashayekhi, M. (2016). Photocatalytic degradation of a textile dye in aqueous phase over ZnO nanoparticles embedded in biosilica nanobiostructure. *Desalination and Water Treatment*, 57(29): 13494-13504.
22. Malwal, D. and Gopinath, P. (2016). Enhanced photocatalytic activity of hierarchical three dimensional metal oxide@CuO nanostructures towards the degradation of Congo red dye under solar radiation. *Catalysis Science & Technology*, 6(12): 4458-4472.
23. Chatti, R., Rayalu, S. S., Dubey, N., Labhsetwar, N. and Devotta, S. (2007). Solar-based photoreduction of methyl orange using zeolite supported photocatalytic materials. *Solar Energy Materials and Solar Cells*, 91(2), 180-190.
24. Menon, S. G., Kulkarni, S. D., Choudhari, K. S. and Santhosh, C. (2016). Diffusion-controlled growth of CuAl₂O₄ nanoparticles: Effect of sintering and photodegradation of methyl orange. *Journal of Experimental Nanoscience*, 11(15), 1227-1241.